Effect of Substrate Hydrophobicity on Surface−Aggregate Geometry: Zwitterionic and Nonionic Surfactants

Lachlan M. Grant and William A. Ducker*

Department of Chemistry, University of Otago, P.O. Box 56, Dunedin, New Zealand

Received: December 9, 1996; In Final Form: April 12, 1997[⊗]

The zwitterionic surfactant, dodecyldimethylammoniopropanesulfonate (DDAPS), and the nonionic surfactant, penta(oxyethylene) *n*-decyl ether ($C_{10}E_5$), both form aggregates (hemimicelles) at the interface between aqueous solution and several covalent solids. DDAPS forms spherical micelles on (hydrophilic) silicon nitride, spherical micelles on (hydrophilic) mica, and hemicylindrical micelles on (hydrophobic) graphite. $C_{10}E_5$ forms globular micelles on silicon nitride and flat sheets on graphite. Thus, both surfactants form lower curvature aggregates on a more hydrophobic substrate. This behavior is interpreted in terms of a lower free energy for the hydrophobic-substrate system when there is minimal contact between water and the hydrophobic substrate. Since the surfactant headgroups have a higher affinity for the hydrophilic substrates, there is also a correlation between the surfactant curvature and the affinity of the headgroup for the solid substrate. The aggregate morphology is not a function of surfactant concentration above the critical micelle concentration, but the repeat distance of the aggregate unit is a weak function of concentration. This behavior is interpreted in terms of the distance dependence of the force between the adsorbed aggregates. The effect of substrate hydophobicity has been investigated for net-uncharged surfactants in order to minimize the effect of the strong monopolar charge−charge interactions that occur for anionic or cationic surfactants.

Introduction

It is well-known that above a critical concentration (the cmc), surfactant molecules associate into aggregates such as micelles or vesicles. This concentration and the structure of the aggregates are functions of the solution conditions and in many cases can be rationalized by considering the intermolecular forces. For some time there has been considerable indirect evidence that surfactants also aggregate at interfaces,[1] but recently it has been found that atomic force microscopy (AFM)[2] can be used to obtain direct images of surface aggregates[3] at the interface between solid substrates and aqueous solutions. It is now possible to perform systematic investigations of the relationship between surface−aggregate structure and the nature of the surfactant and the interface and thus to understand the aggregate shape in terms of intermolecular forces. Our aim is to investigate the role of the interaction between the solid substrate and the solvent by examining adsorption on substrates of different hydrophobicity. In previous work it was suggested that the shape of surface aggregates is strongly influenced by the interaction between the two bulk phases.[4] The existence of relatively weak forces between the solvent molecules and the substrate surface is a driving force for surfactants to replace solvent molecules at the surface (i.e., to create a surface excess). Since different arrangements of surfactants at an interface replace different areas of the interface per surfactant molecule, it is natural to consider whether different aggregate shapes form in response to a change in the bonding across the interface. The current work is an extension of previous study of the adsorption of a zwitterionic surfactant at a single concentration.[5]

The final state of a surface aggregate is a balance between many forces including those that dictate the structure of aggregates in bulk solution: e.g., (1) the force to reduce the contact between water and the hydrophobic chains of the surfactant (the hydrophobic effect); (2) the favorable interactions between the headgroups and the solvent; (3) interactions between different headgroups within a surfactant aggregate (usually repulsive); (4) constraint on optimizing the above three forces due to the fixed relative proportion and geometric arrangement of the hydrophilic and hydrophobic portions (packing constraints); (5) entropy of mixing that favors smaller aggregates. At an interface between a solid and aqueous solution there are additional interactions between the solid and the solution and between the solid and both the hydrophilic and hydrophobic portions of the surfactant. One manifestation of these is that the solid substrate usually acts to concentrate the surfactant, so that the local mole fraction of surfactant is much higher than that in bulk solution.

To simplify this array of factors, we have studied only net-uncharged surfactants. The interaction between monopoles occurs over a long range and so is more strongly affected by solution conditions or by neighboring aggregates. We have studied the surface aggregation of dodecyldimethylammoniopropanesulfonate (DDAPS), a zwitterionic surfactant, or penta(oxyethylene) *n*-decyl ether ($C_{10}E_5$), a nonionic surfactant, when each is adsorbed to graphite, mica, or silicon nitride. Graphite is hydrophobic and silicon nitride and mica are hydrophilic, so this study allows us to consider the role of the interaction between the solvent and the solid substrate. Naturally, a change in the solid substrate also leads to changes in the interaction of the surfactant molecules with the solid substrate, so we are forced to consider these two interactions together.

Previous work has shown that the cmc's of DDAPS[6,7] and $C_{10}E_5$[8] are 3 and 0.9 mM, respectively, at 25 °C; the current work focuses on concentrations near or above the bulk cmc. Graphite can be cleaved to produce a smooth basal plane consisting of aromatic carbon atoms that are chemically inert in the aqueous solutions studied here. Mica can also be cleaved to form a molecularly smooth aluminosilicate layer, which is inert in solution except that potassium ions dissociate from the lattice. The dissociation leaves negative sites that can bind other cations, notably H^+ in aqueous solution.[9] The nature of the silicon nitride surface depends on the method of preparation.

[⊗] Abstract published in *Advance ACS Abstracts,* May 15, 1997.

S1089-5647(96)04014-X CCC: $14.00

A previous X-ray photoelectron spectroscopy (XPS) study of silicon nitride substrates produced in the same manner as those used here revealed a surface consisting of a mixture of acidic SiOH and basic $SiNH_2$ groups[10] (which are also potential hydrogen-bonding sites). The point of zero charge (PZC) is about pH 6.[10]

Methods

Sample Preparation. Water was prepared by distillation then passage through a Milli-Q RG system consisting of charcoal filters, ion-exchange media, and a 0.2 μm filter. The resulting water has a conductivity of 18 MΩ cm^{-1} and a surface tension of 72.4 mJ m^{-2} at 22.0 °C. Dodecyldimethylammoniopropanesulfonate (DDAPS, 98%) was obtained from Aldrich Chemical Co. DDAPS sometimes contains a low concentration of contaminants, which cause a minimum in the surface tension as a function of concentration and a change in the morphology of aggregates adsorbed to mica.[14] DDAPS used in the experiments reported here was purified by recrystallization from distilled 2-propanol and did not exhibit a minimum in the surface tension. The cmc of the recrystallized DDAPS was 3.0 mM as determined by the intersection of the two linear regions in a plot of ^{1}H NMR chemical shift as a function of inverse concentration. Penta(oxyethylene) *n*-decyl ether ($C_{10}E_5$), obtained 97% pure from Sigma Chemical Co. was used without further purification. A fresh solid substrate was prepared in a laminar flow cabinet immediately before each experiment in the following manner: adhesive tape was used to cleave along the basal plane of graphite from a pyrolytic graphite monochromator (grade ZYH, Union Carbide); tweezers were used to cleave along the basal plane of muscovite mica; and a piece of silicon wafer with a 210 nm surface layer of silicon nitride prepared by low-pressure chemical vapor deposition (Silica Source Technology Corp., Tempe, AZ) was exposed to UV irradiation for 40 min (~9 mW cm^{-2} at 253.7 nm). The advancing water contact angle of these substrates was 90°, <10°, and <10° for graphite, mica, and silicon nitride, respectively. Neither the mica nor the silicon nitride was completely wetted by water.

Microscopy. Images were captured using a Nanoscope III AFM (Digital Instruments, CA) using silicon ultralevers (Park Scientific, CA) with a spring constant of 0.12 ± 0.02 N m^{-1}, as determined by measuring the resonant frequency of loaded and unloaded cantilevers.[23] The ultralevers were irradiated for 40 min (~9 mW cm^{-2} at 253.7 nm) in a laminar flow cabinet before use. All images presented are deflection images (showing the error in the feedback signal) with integral and proportional gains of about 1−4 and scan rates of 10 Hz. No filtering of images was performed other than that inherent in the feedback loop. Distances in lateral dimensions were calibrated by imaging a standard grid (2160 lines/mm), and distances normal to the surface were calibrated by measuring etch pits (180 nm deep). All measurements were performed in the temperature range 25 ± 2 °C and in equilibrium with single-phase surfactant solutions. For each solution condition, the cell (volume ~ 0.1 mL) was rinsed with several milliliters of solution over about 10 min, then after a further 10 min equilibration, the force between the tip and sample was measured, partly to determine the force at which the adsorbed surfactant could be imaged. In the presence of adsorbed surfactant, there was always a stable imaging position when the tip and sample were separated by a few nanometers, and the images were captured when the setpoint was adjusted so that the tip maintained this position.[11] Since this force is due to the surfactant, the image shows the structure of the surfactant layer.

Force Measurement. The forces between the tip and sample were also measured using a Nanoscope III AFM and analyzed as described previously.[12] It is important to note that the zero of distance is defined to occur when the gradient of the force has a high and constant (negative) value, which implies that the tip is in contact with the sample. Very strongly adsorbed material may not be displaced in a particular measurement, and therefore there may be a systematic error in evaluating the zero of separation for each complete measurement of force as a function of separation. The zero of force is defined to occur when the gradient in force is very low at a large separation. Thus it is possible to miss a slowly varying force which may have considerable magnitude. This problem is compounded by optical interference between reflected light from the cantilever and substrate that is inherent to the light lever detection device used in the Nanoscope III and often leads to a slight variation in the apparent force with distance even when the tip is at a large distance from the substrate.

The measured force depends on the shape of the tip. Since we have used different tips for different experiments, the magnitude of the forces for various substrate/surfactant combinations are not comparable.

Results

Figure 1 shows three AFM deflection images of the interface between silicon nitride and aqueous 4.4 mM penta(oxyethylene) *n*-decyl ether 5 ($C_{10}E_5$) solution and the force acting on the tip as it approaches the interface in a normal direction. Contrast in an AFM image arises from a gradient in force on a tip as a function of distance from the substrate, so the resultant image is a function of the applied force. In this case, when the tip approaches the interface from a large separation there is a weak but measurable repulsive interaction starting at about 5 nm separation and then a strong repulsion at 2 nm. Rutland and Senden have previously measured the force between $C_{12}E_5$-coated *silica* surfaces.[13] They observed a barrier at 4 nm, which is consistent with our measurements if the barrier in the current experiments is due to removal of surfactant from the silicon nitride substrate only. When the applied load exceeds a critical limit, the separation decreases to a constant value (defined as zero separation) over a very small load range. If the load is decreased before this critical value, the force−distance relation is almost reversible, but after exceeding this limit, the load must be decreased to a lower threshold before the separation increases. This hysteresis is common in force measurement and is due to the mechanical instabilities caused by the finite stiffness of the measurement spring. For $C_{10}E_5$ on silicon nitride, the force−distance relationship displays additional hysteresis—the entire outward curve is displaced to smaller separations for a given load—indicating measurably slow kinetics for the rearrangement of surface structures. Our interpretation of the force−distance relationship is that, starting at about 4−5 nm separation between the tip and sample, the tip interacts with weakly bound or easily compressed surfactant. At 2 nm separation there is a more strongly bound or more dense layer which is displaced at a load of about 5 nN, above which the tip contacts the silicon nitride substrate. The images that we record are then interpreted according to this model: when the force is attributed to the adsorbed surfactant then the image is attributed to the adsorbed surfactant. At low force (Figure 1a) we record ill-defined patches, but definitely a force field that is laterally inhomogeneous. At a higher force (Figure 1b), we observe globular objects (~6 nm in size) covering the surface, superimposed on a background of larger scale (50 nm) features. On reexamining (a) (or a Fourier transform of (a)), we see that globular objects

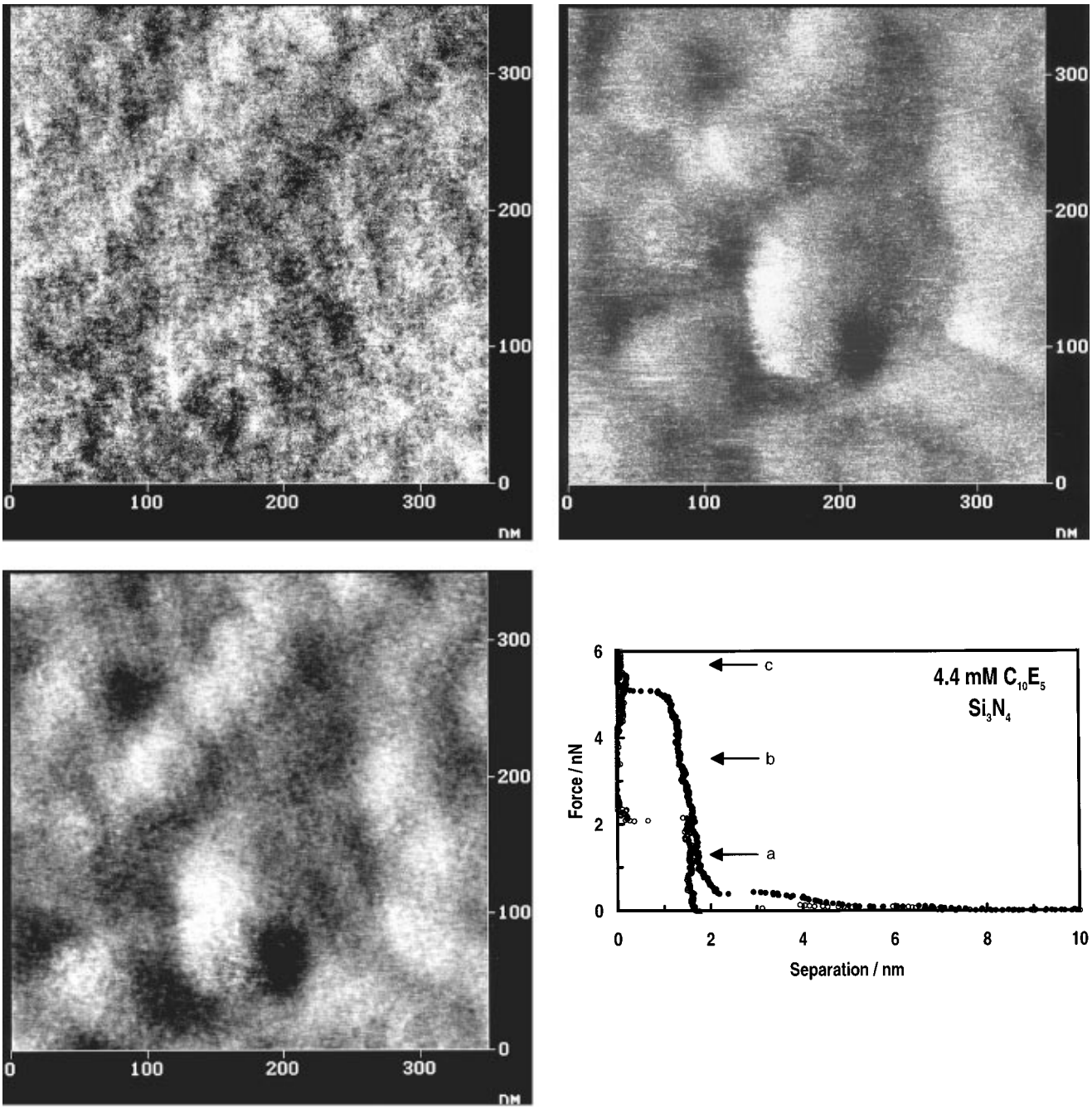

Figure 1. AFM deflection images of globular $C_{10}E_5$ aggregates adsorbed to the interface between a 4.4 mM solution and silicon nitride at a variety of forces: (a, top left) low force, ~0.5 nN, revealing some aggregate structure, (b, bottom left) medium force, ~2 nN, revealing adsorbed aggregates on an undulating substrate, and (c, top right) high force, ~4 nN, revealing the features of the underlying substrate. (d, bottom right) Force between an (oxide coated) silicon tip and silicon nitride in 4.4 mM $C_{10}E_5$. The closed circles represent forces on approach of the tip and sample, and the open circles represent forces on separation. The labeled arrows show the approximate force for each image.

of the same size were visible at lower force. The higher resolution in (b) is probably due to a larger gradient in the force and a closer proximity of the tip to the imaged structures. At a force that exceeds the threshold required to achieve our zero of separation, features on the 6 nm length scale are no longer visible and we image only the 50 nm features, which we interpret to be the underlying silicon nitride substrate. Comparison with (b) confirms that the same substrate features are clearly visible before the tip contacts the substrate. (Similar features are imaged in pure water.) Of the noncontact images, Figure 1b provides us with the clearest image of the adsorbate structure: globular "hemimicelles" about 6 nm in diameter and 2 nm in depth adsorbed on an undulating substrate. This structure is measured when the surfactant is confined between a tip and solid substrate under a load of between 1 and 5 nN, and there is the possibility that the structure may be different in the absence of the tip. A similar structure was also observed just below and just above the cmc, in 0.6 and 1.9 mM $C_{10}E_5$, respectively.

In previous work on other surfactants (e.g., ref 4), we have found that the surface aggregates form with a distinct period. A Fourier transform of images of $C_{10}E_5$ does not produce a clear maximum in the period but instead a diffuse region of moderate intensity starting at about 5 nm with no obvious upper limit. This may be due to either polydispersity in the size of the aggregates or a weak gradient in the force between the adsorbed aggregates.

Figure 2a shows the structure of the adsorbed aggregates on graphite at the same bulk concentration as in Figure 1 (4.4 mM). Figure 2b shows the force acting on the tip as it approaches the

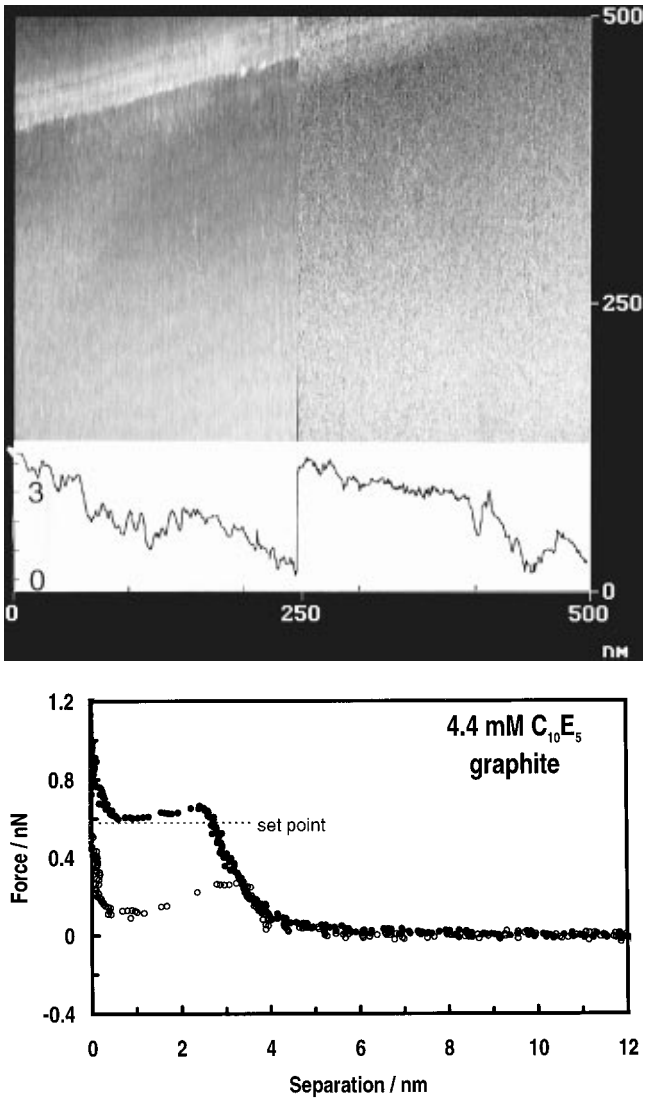

Figure 2. (a, top) AFM deflection images of $C_{10}E_5$ adsorbed to the interface between a 4.4 mM aqueous $C_{10}E_5$ solution and silicon nitride. The left side is an image of the underlying substrate, and the right side is an image of the adsorbed surfactant. The trace at the bottom shows a cross section through the height image. For the image, the scale in both dimensions is identical and indicated at the bottom; for the cross section, the vertical scale is shown at the left axis and is highly exaggerated. There is a step in the graphite running across top of the image. When $C_{10}E_5$ adsorbs to graphite, it forms a film with no lateral features resolved in our experiments. Our conviction that the right side is an image of an adsorbed film comes from three pieces of evidence: (i) the force curve is different from that measured in the absence of $C_{10}E_5$, (ii) we are imaging at a force at which the tip is slightly separated from the graphite in a normal force measurement, and (iii) a slight increase in the force results in the tip moving approximately 3 nm closer to the graphite. This is shown by the 3.2 nm jump in the cross section through the height image shown below the deflection image. This displacement before hitting the substrate indicates that the tip was previously on the surfactant layer. (b, bottom) Force between the tip and sample. The dotted line shows the approximate setpoint for Figure 2a.

graphite substrate and is similar in general features to that shown for silicon nitride in Figure 1d. (The magnitude of the force cannot be compared to that in Figure 1d because a different tip was used.) The image was captured at a force very close to the point of mechanical instability. Under this condition, small fluctuations in applied force due to temperature fluctuations or small variations in the critical force will allow the tip to move onto the branch of the force−separation relation which is at zero separation. The right side of the image was captured first, when the tip was on the finite-separation branch of the force−separation relation, and the left side was captured after the tip crossed to the zero-separation branch. The right side is thus an image of the adsorbate, and the left is an image of the graphite substrate. The adsorbate structure shows no lateral inhomogeneity. When imaged on a scale of $(800\ \text{nm})^2$ down to $(50\ \text{nm})^2$, it was similarly devoid of features.

It is important to ensure that it is actually the adsorbate that is measured and not the solid substrate below or the solution above, both of which are laterally featureless on the time and length scales explored. Our conviction that the measurements were performed on the adsorbed layer arises from three conditions: (1) The force−separation relation was different from that measured in water, indicating that adsorption had occurred. A barrier was observed at 2−4 nm, the lower limit of which corresponds to the extended length of a $C_{10}E_5$ molecule. (2) When the tip jumped to the substrate branch of the force−separation relation, the "jump" was about 2−3 nm, indicating that previously the tip was measuring on a layer above the surface. This is shown by cross section through the "height image" which was captured simultaneously with the deflection image. The displacement is consistent with the length of the surfactant molecule. (3) The feedback setpoint was maintained so that at the start of the image the imaging force was just below the instability force (at 0.30−0.35 nN). This combination of force and distance is unique to a tip position on the layer and was met for many images over different length scales. Similar behavior was observed for 0.6, 1.9, and 4.4 mM $C_{10}E_5$ solutions. In each case they provide strong evidence that the adsorbed layer is laterally homogeneous.

When the force curve on graphite is compared to the curve on silicon nitride in more detail, it is apparent that the force on graphite increases more steadily, and reaches a mechanical instability at about 2.5 nm separation. On silicon nitride, the force increases in two distinct regimes, and the instability is reached only at about 1.2 nm. It is also interesting to note that in both cases, the "jump" of the tip from the surfactant layer onto the substrate is very slow (indicated by the measurement of several points during the "jump"). This suggests that rearrangement times for the surfactant molecules are similar to the travel time for the tip and measurably slower than rearrangement times for other surfactants (e.g., DDAPS).

The organized structure of DDAPS at the interface between 3, 10, 50, and 250 mM aqueous DDAPS solutions and graphite, mica, or silicon nitride was also measured. For mica and silicon nitride, the surfactant always adsorbed in aggregates where the two dimensions parallel to the interface were similar (5−6 nm), and for graphite, one dimension was always very long (>100 nm) and the other was about 5−6 nm. Figure 3 shows typical images in 10 mM bulk DDAPS solutions, which are similar to those in ref 5. Fourier transforms of each image revealed that the value of the dominant period in each image was a weak function of concentration (Figure 4). For both mica and silicon nitride, the dominant period decreased as the concentration increased. For mica, this change is shown in Figure 4; for silicon nitride, the change was similar (the period decreased by about 1 nm with the largest change between 3 and 10 mM) but the absolute values of the period varied significantly from experiment to experiment. If the dominant frequency represents the sum of the diameter and the spacing between the aggregates,[14] then the decrease in period means that either the aggregates are becoming smaller or they are moving closer together. It is reasonable to expect a higher density of surfactant (which is in accord with a smaller separation between the aggregates) as the chemical potential of the surfactant rises, but

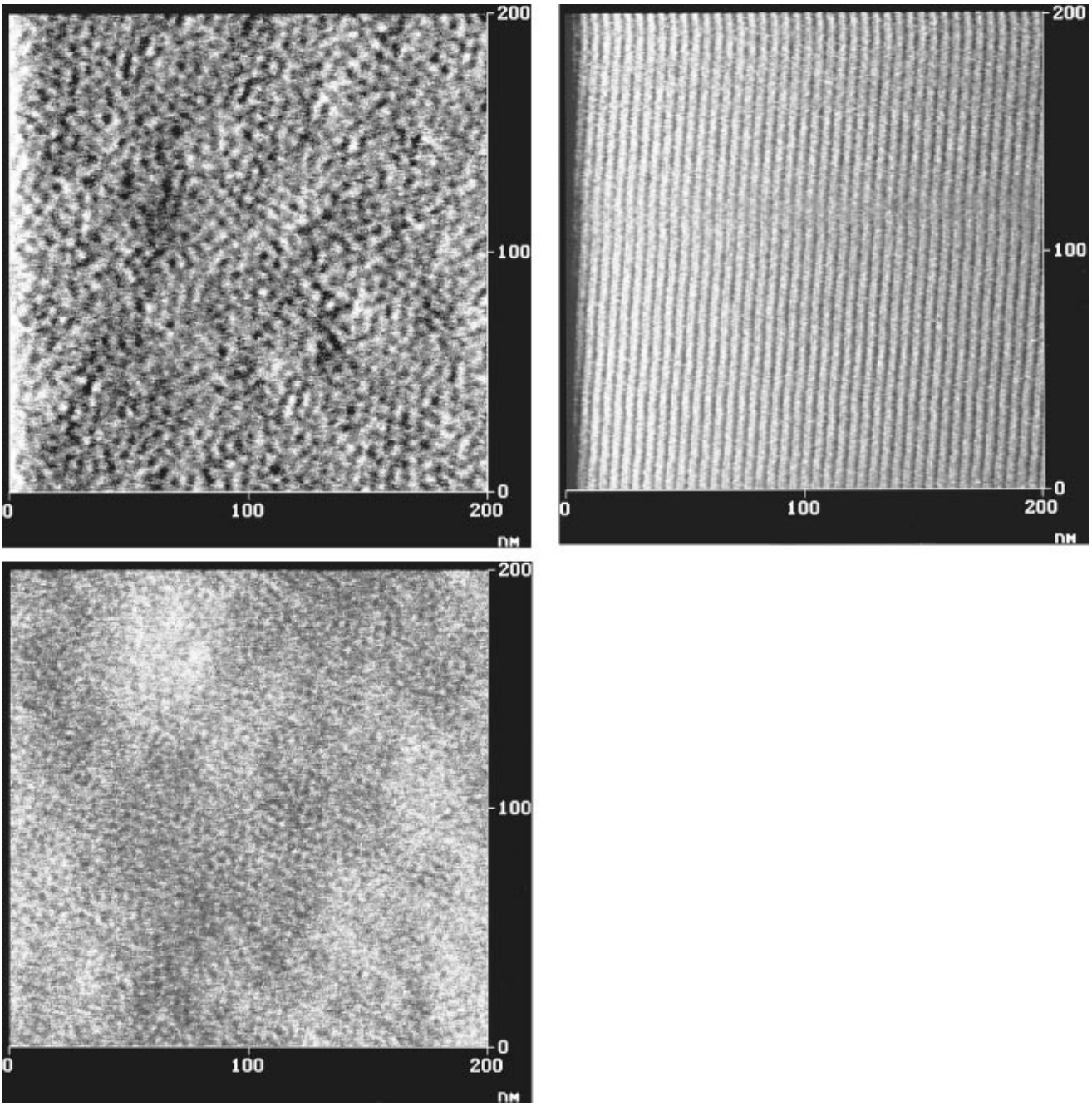

Figure 3. AFM images of DDAPS adsorbed to the interface between 10 mM DDAPS solution and (a, top) mica, (b, middle) silicon nitride, and (c, right) graphite. Aggregates adsorbed to mica and silicon nitride have two similar dimensions (4−6 nm) in the plane of the interface whereas aggregates adsorbed to graphite have one dimension that is much longer than the other.

it is interesting that a measurable effect occurs during the small chemical potential change above the cmc.

While the effect of surfactant concentration in the solution phase was only a weak influence on the observed AFM image, it exerted a strong influence on the measured force between the tip and the sample. Figures 5 and 6 show the force for silicon nitride and mica, respectively. For silicon nitride in 3 mM DDAPS, the force is measurably attractive at about 8 nm separation between the tip and silicon nitride and then becomes repulsive at a separation of about 3.3 nm. When the force is increased from this point, the separation decreases slowly up to a yield force, at which point the tip jumps toward the surface. The barrier from 3.9 to 2.6 nm shows the thickness of the adsorbed structures as a function of load and indicates that there is again a critical load above which the surfactant is displaced. There is some evidence to suggest that the surfactant may only move laterally, and not into the bulk solution,[14] so this value does not necessarily represent the desorption force. When the concentration of surfactant in solution is increased to 10 mM, the magnitude of the barrier required to displace the surfactant increases, and there is a decrease in the range of the attractive force at greater separations. The images shown in Figure 3 were captured near the minimum in force (at about 3.5 nm separation) with the desire to cause the minimum influence on the adsorbed layer. At 50 mM, the force required to eject the layer adjacent to the silicon nitride is similar to that in 10 mM, but there is also a barrier at about 7 nm, showing the formation of another layer of similar thickness. At 250 mM there are three distinct force barriers, suggesting that there are three layers of micelles between the tip and silicon nitride (and a less distinct fourth barrier). The removal of each successive layer requires more force and a higher force gradient, perhaps indicating an increase in organization as the film thins. The behavior of DDAPS adsorbed to mica is very similar (Figure 6) and the data for the

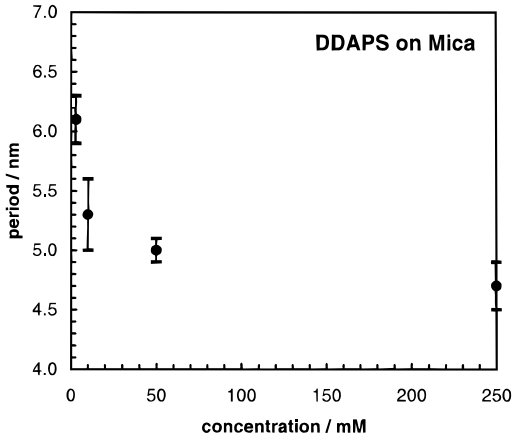

Figure 4. Period of DDAPS aggregates adsorbed to mica. Each period is the average value of the density maximum from Fourier transforms of many $(400\ nm)^2$ AFM images. The lowest measured concentration is the cmc (3 mM).

TABLE 1: Tip−Sample Separation (nm) of Maxima and Minima in the Force

DDAPS	F_{max}		F_{min}	
(mM)	mica	silicon nitride	mica	silicon nitride
3	2.8	2.6	4.45	3.9
10	2.5	2.6, 7.2	3.9, ∼8	4.1
50	3, 7.8, 11.8	2.6, 7.1	5.1, ∼9	4.4, 8.6
250	2.9, 7, 12.2	2.3, 6.5, 10.2	3.7, 8.5, 15	3.8, 8.3, 12.5

maximum and minimum force in the oscillations are shown in Table 1. ^{1}H NMR measurements show that the hydrodynamic diameter of DDAPS micelles is 4.92 nm,[15] and fluorescence measurements show that the aggregation number of DDAPS in solution remains approximately constant at 65 per micelle over the range 7−200 mM,[16] and hence the diameter is approximately constant over the same range. We have measured the layer thickness as a function of force, so there is no unique diameter, but even at the minimum in force, the thickness is smaller than the hydrodynamic diameter. Previously, an oscillatory force curve has been reported for hexadecyltrimethylammonium bromide (CTAB) solutions between macroscopic mica sheets.[17] In that case, the period was larger, and this was ascribed to the larger effective micelle radius because of electrostatic repulsions between the micelles.

The existence of multilayers of micelles is not unreasonable if there is an attractive force between the micelles. Attard has calculated the force between two planar arrays of dipoles each at the interface between a high and low dielectric medium.[18] The force has attractive contributions due to van der Waals forces (between the bulk phases and due to correlations between the dipoles) and repulsive forces due to image charges. Unfortunately, it is difficult to apply Attard's work to our observations because the calculated force was very sensitive to the distance between the charges in the dipole, to the position of the dipole relative to the dielectric discontinuity, and also to the degree of free rotation of the dipolar headgroup. Undoubtedly there is some free rotation of the headgroup for DDAPS, but covalent attachment of the cation closer to the alkyl chain forces some alignment of the negative end of the dipole away from the micelle core. The facts that these quantities are unknown and the geometry is highly curved in our system make it impossible to determine even the sign of the interaction from his work. However, the forces between a silicon nitride AFM tip and a silicon nitride substrate have been measured in the presence of DDAPS solutions.[5] In this case the force was attractive in the range 5−15 nm, and it is likely that both

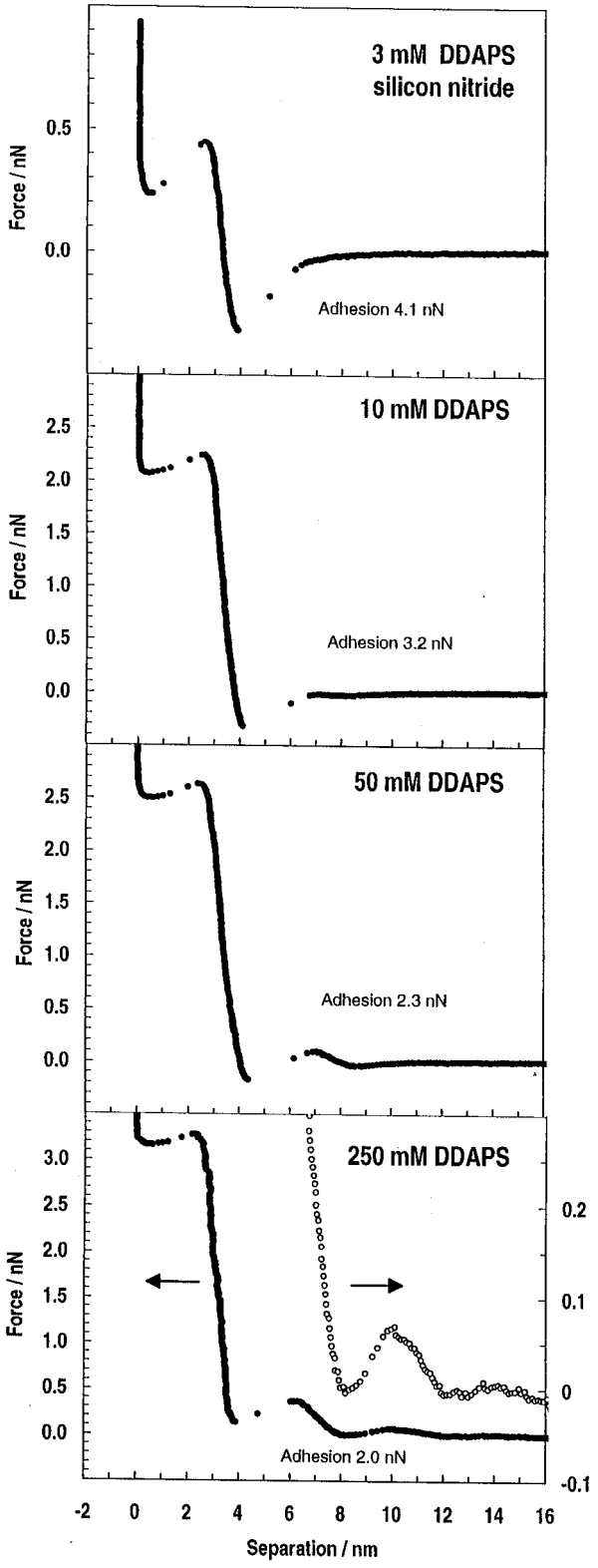

Figure 5. Force between an oxide-coated silicon AFM tip and silicon nitride in aqueous DDAPS solutions. For 250 mM DDAPS, the open circles represent the same data points with the force axis translated and magnified 10×. The four curves were measured with the same tip so the magnitudes are comparable.

surfaces are similarly coated in surfactant. There will be some contribution due to van der Waals forces from the underlying substrate, but at small separations the force is dominated by the adsorbate because of the smaller separation between the adsorbate atoms. The measured attractive force between surfactant layers is consistent with the formation of multilayers observed here.

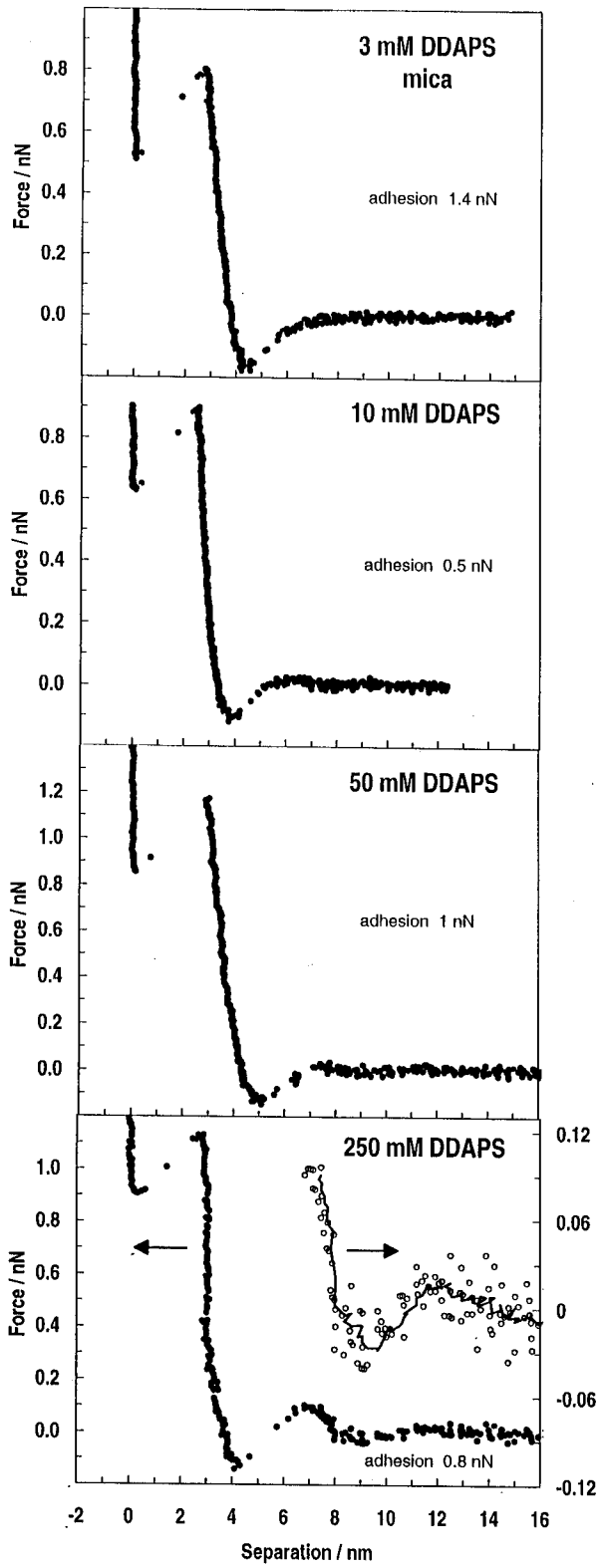

Figure 6. Force between an oxide-coated silicon AFM tip and mica in aqueous DDAPS solutions. The 3 and 10 mM data were captured with one tip, and the 50 and 250 mM were captured with another. For 250 mM DDAPS, the existence of a third oscillation in the force−distance profile is shown more clearly by the open circles, which are the same data points, displayed with the force axis translated and magnified. The solid line is a seven-point moving average.

Discussion

Role of the Solid Substrate. Table 2 shows a summary of the structure of adsorbed aggregates on the various substrates. Both surfactants form aggregates that are similar to the bulk-solution structure on the hydrophilic substrates, but on the hydrophobic substrate a lower curvature structure is formed (Figure 7). For DDAPS, the lower curvature structure is hemicylinders, and for $C_{10}E_5$ it is flat sheets. This phenomenon can be explained on the basis of the lack of any high-energy bonds between graphite and water: the free energy of the system is reduced when the surfactant covers more of the graphite−solution interface, or more per surfactant molecule.

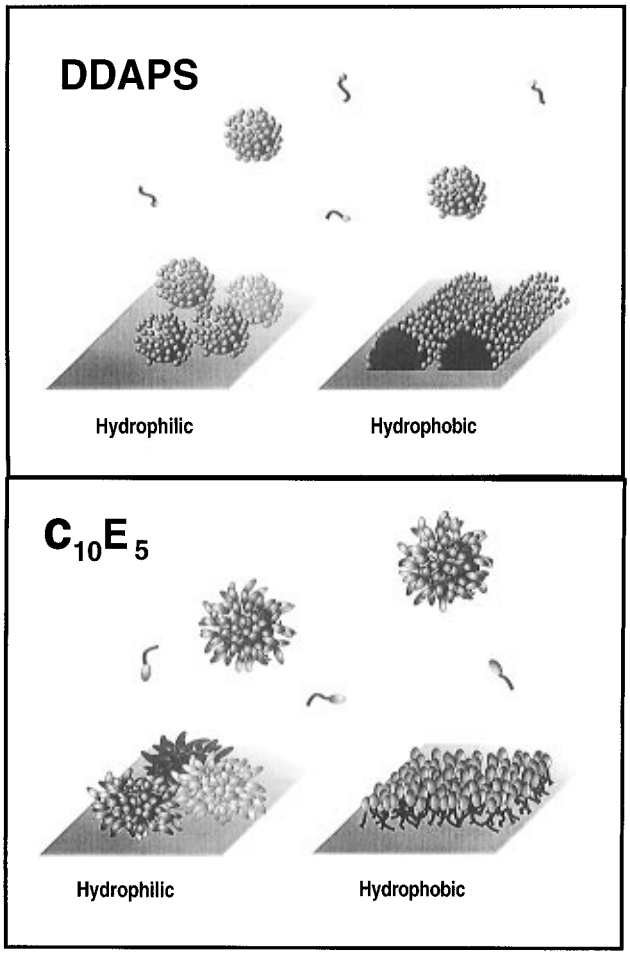

Figure 7. Schematic figure showing the surfactant aggregates adsorbed to the solid−solution interface. The aggregate curvature is lower on the hydrophobic substrate for both surfactants, but the actual structure is different: hemicylinders for DDAPS and a flat sheet for $C_{10}E_5$. The structure may depend on the details of the interactions for each substrate−surfactant pair: other hydrophobic and hydrophilic substrates may produce different surface-aggregate shapes.

TABLE 2: Structure of Adsorbed Aggregate above the (Bulk) Cmc

	silicon nitride	mica	graphite
DDAPS	~spherical micelles	~spherical micelles	hemicylinders
$C_{10}E_5$	polydisperse and flattened micelles	no adsorption	flat layer

We have demonstrated a correlation between the interfacial energy and the curvature of the adsorbed aggregates, but clearly the interaction between the substrate and the solvent is only one component of the total interaction. The interaction between the surfactant and substrate is also important. A salient example of this is fact that ethylene oxide surfactants either do not adsorb to mica or adsorb very weakly even at concentrations many times the cmc[19] but adsorb readily to silica below the cmc.[20] Previous workers have found that a hydrogen-bonding substrate is required for C_xE_y adsorption.[19,21] Surface silanol and silolamine groups on the silicon nitride are available for hydrogen bonding on the silicon nitride surface, so the observed adsorption

of ethylene oxides is consistent with this idea. Forces exerted by the graphite surface on the surfactant also influence the aggregate structure. On the gross scale, steps and irregularities cause an interruption to the long, thin aggregates that are observed on graphite. It has been suggested that the steps in the graphite, which are aligned with the crystal lattice, are nucleation sites for formation of the aggregates and are responsible for the observation that the long axis of surfactant aggregates on graphite is always aligned in one of three directions.[4] An alternate suggestion is that there is some particular local interaction that leads to one of three particular orientations.[3] Our force measurements lend some support to the second hypothesis. It is very common to observe a barrier in the force curve at about 0.2−0.3 nm separation between the tip and graphite. This can be seen in the force on DDAPS and sodium dodecyl sulfate[4] and surprisingly even for $C_{10}E_5$. A reasonable explanation for a barrier of this thickness is that there is a layer of surfactant lying parallel to the surface, in contact with the graphite, that is held more strongly than the rest of the adsorbed micelle, not just by the nonspecific hydrophobic interaction. When a force is applied to a hemicylinder, sometimes all but this parallel layer is displaced in one step and the bottom layer is removed in a second step. When imaging on graphite, it is common to continue to observe a structure that is very similar to the normal "hemicylindrical" structures even after the force exceeds the mechanical instability, which we attribute to the displacement of the aggregate in a normal-force measurement. Using the above model, this is explained by the tip imaging a single layer of adsorbed molecules in contact with and parallel to the graphite surface. If this layer is more strongly held then it will also be the first adsorption site and thus the nucleation site and template for the formation of the hemicylinders. It is more difficult to use a similar explanation for steps in the $C_{10}E_5$ force curve since the proposed structure does not contain a layer of molecules lying parallel to the interface. To explain the force curve there must either be a layer of molecules parallel to the interface lying under the approximately perpendicular monolayer, or a transformation from a perpendicular to a parallel layer under the applied load and geometrical restrictions imposed by the tip.

It is interesting to consider the surface aggregate structure in terms of perturbations of the solution-aggregate structure due to the replacement of water−headgroup interactions and water−solid interactions with water−water interactions and surfactant−solid interactions. If the solid can form one to a few high-energy bonds with the surfactant headgroups, then it is reasonable to have slightly perturbed micelles attached to the solid. This is the proposed structure for DDAPS on mica or silicon nitride. A high density of surface sites that can form strong bonds between the headgroups and the substrate will lead to the formation of many bonds between the surface "micelle" and the substrate and a strong perturbation of micelle structure. Thus a less curved micelle would form as the density of available strong-bonding sites increases if the interaction of the headgroup with the substrate is sufficient to overcome the forces that lead to the curvature in bulk solution.

If the solid substrate cannot form hydrogen bonds with water or with the surfactant headgroup, then a large free energy reduction of the system is possible by covering up the solid substrate with surfactant hydrocarbon tails. This free energy might be so great as to force the headgroups closer together than in solution micelles and/or to force the hydrocarbon chain to spend more time in shorter length configurations. In either case, the surfactant behaves as if it has a higher packing parameter, and the curvature of the aggregate drops. For DDAPS on graphite this was observed as hemicylinders, and for $C_{10}E_5$, as a monolayer.

Comparison to Measurements on Hydrophobic and Hydrophilic Silica. Tiberg and co-workers have studied the adsorption of a range of poly(ethylene oxide) surfactants on hydrophilic and hydrophobic silica using ellipsometry.[20,21] Although the solid substrates and surfactants are different, the system is sufficiently similar to allow comparison to our results for $C_{10}E_5$ on graphite and silicon nitride. Tiberg finds that the adsorbed thickness and the surface excess of $C_{14}E_6$ on hydrophilic silica increase dramatically just below the cmc and interprets this in terms of surface aggregation into micelle-like structures.[20] On hydrophobic silica, the adsorbed thickness and surface excess rise much more slowly, in accord with a Langmuir isotherm, indicating a noncooperative association. He interprets this steady increase in density as a continuous film in which the poly(ethylene oxide) headgroups decrease their tilt relative to the surface normal.[20] Tiberg's results and conclusions are thus consistent with our images of an aggregated structure on (hydrophilic) silicon nitride and a laterally homogeneous film on (hydrophobic) graphite.

Conclusions

The organization of net-uncharged surfactants at interfaces is strongly influenced by the nature of the interface. Organization into a laterally homogeneous layer has been observed for $C_{10}E_5$ on graphite, but on silicon nitride, which is relatively hydrophilic and has sites for hydrogen bonding to $C_{10}E_5$, the surfactant aggregates into discrete surface micelles over a concentration range of two-thirds to twice the cmc. For DDAPS, surface micelles are observed on the hydrophilic silicon nitride and hemicylinders are observed on hydrophobic graphite.

Interactions between the hydrophilic substrate and water will lower the free energy of the system more than interactions of the hydrophobic substrate with water. The free energy of the hydrophobic-substrate system can be reduced if the area exposed to water can reduced by covering it with surfactant. For a given surfactant density, less curved substrates (e.g., monolayers or hemicylinders) will replace more solid−solution interface than highly curved aggregates such as micelles or half-micelles. When the amount of surfactant is no longer limiting, a flat sheet will also cover more surface than curved structures.

For DDAPS on mica or silicon nitride, several layers of micelles form in the thin film between an AFM tip and the flat substrate.

References and Notes

(1) For example: Chandar, P.; Somasundaran, P.; Turro, N. J. *J. Colloid Interface Sci.* **1987**, *117*, 31−45. Wakamatsu, T.; Fuerstenau, D. W. In *Adsorption from Aqueous Solution*; Weber, W. J., Matijevic, E., Eds.; American Chemical Society: Washington, DC, 1968; pp 161−172. Hunter, R. J. *Foundations of Colloid Science*; Oxford University Press: Oxford, 1989; Vol. II, Chapter 12.

(2) Binnig, G.; Quate, C.; Gerber, G. *Phys. Rev. Lett.* **1986**, *56*, 930−933.

(3) Manne, S.; Cleveland, J. P.; Gaub, H. E.; Stucky, G. D.; Hansma, P. K. *Langmuir* **1994**, *10*, 4409−4413.

(4) Wanless, E. J.; Ducker, W. A. *J. Phys. Chem.* **1996**, *100*, 3207−3214.

(5) Ducker, W. A.; Grant, L. M. *J. Phys. Chem.* **1996**, *100*, 11507−11511.

(6) Weers, J. G.; Rathman, J. F.; Axe, F. U.; Crichlow, C. A.; Foland, D. R.; Scheuing, D. R.; Wiersema, R. J.; Zielske, A. G. *Langmuir* **1991**, *7*, 854−867.

(7) La Mesa, C.; Sesta, B.; Bonicelli, M. G.; Ceccaroni, G. F. *Langmuir* **1990**, *6*, 728−731.

(8) van Oss, N. M.; Hak, J. R.: Rupert, L. A. M. *Physicochemical properties of selected anionic, cationic and nonionic surfactants*; Elsevier: Amsterdam, 1993; p 214.

(9) Claesson, P. M.; Herder, P.; Stenius, P.; Eriksson, J. C.; Pashley, R. M. *J. Colloid. Interface Sci.* **1986**, *109*, 31−39.
(10) Senden, T. J.; Drummond, C. J. *Colloids Surf.* **1995**, *94*, 29−41.
(11) Ducker, W. A.; Clarke, D. R. *Colloids Surf. A* **1994**, *94*, 275−292.
(12) Ducker, W. A.; Senden, T. J.; Pashley, R. M. *Langmuir* **1992**, *8*, 1831−1836.
(13) Rutland, M. W.; Senden, T. J. *Langmuir* **1993**, *9*, 412−418.
(14) Ducker, W. A.; Wanless, E. J. *Langmuir* **1996**, *12*, 5915−5919.
(15) Faucompré, B.; Lindman, B. *J. Phys. Chem.* **1987**, *91*, 383−389.
(16) Lianos, P.; Zana, R. *J. Colloid Interface Sci.* **1981**, *84*, 100−107.
(17) Richetti, P.; Kékicheff, P. *Phys. Rev. Lett.* **1992**, *68*, 1951−1954.
(18) Attard, P.; Patey, G. N. *Phys. Rev. A* **1991**, *43*, 2953−2962. Jönsson, B.; Attard, P.; Mitchell, D. J. *J. Phys. Chem.* **1988**, *9*, 5001−5005.
(19) Rutland, M.; Christenson, H. K. *Langmuir* **1990**, *6*, 1083−1087.
(20) Tiberg, F. *J. Chem. Soc., Faraday Trans.* **1996**, *92*, 531−538.
(21) Rupprecht, H. *Prog. Colloid Polym. Sci.* **1978**, *65*, 29.
(22) Tiberg, F.; Jönsson, B; Tang, J. A.; Lindman, B. *Langmuir* **1994**, *10*, 2294−2300.
(23) Cleveland, J. P.; Manne, S.; Bocek, D; Hansma, P. K. *Rev. Sci. Instrum.* **1993**, *64*, 403−405.